Proceedings of the
9th Graz Brain-Computer Interface Conference 2024
10.3217/978-3-99161-014-4-022

INVESTIGATING COORDINATES REPRESENTATION DURING REACHING VIA LOW-FREQUENCY EEG: A PRELIMINARY STUDY

Nitikorn Srisrisawang[1], Gernot R. Müller-Putz[1,2]

[1]Institute of Neural Engineering, Graz University of Technology, Graz, Austria
[2]BioTechMed Graz, Graz, Austria

E-mail: gernot.mueller@tugraz.at

ABSTRACT: Understanding how the brain plans reaching movements is crucial in designing a brain-computer interface (BCI) system for motor control. It is still unclear which referencing frame the brain uses to plan the movement. In this study, we investigated the global representation of a referencing frame during reaching planning via a low-frequency electroencephalogram (EEG). Participants were asked to perform directional reaching inward (from the outer target towards the center point) and outward (from the center point towards the outer target) while maintaining gaze on a target such that the reaching in inward and outward conditions should be represented similarly in eye-centered coordinates but differently in shoulder-centered coordinates. We could classify the direction with a peak accuracy of 40.59% but not the inward and outward conditions. The preliminary results confirmed that low-frequency EEG may be globally represented in the eye-coordinates. The classification results suggested that the difference between inward-outward conditions was negligible in low-frequency EEG and could be combined in further analysis.

INTRODUCTION

When reaching for objects (e.g., a glass of water), our brain must rely on sensory information from several sources to execute the reaching. First, the brain must locate the target and the hand via visual and kinematic information. The displacement and direction between the target and the hand can be calculated, and the reaching can eventually be executed.

The evidence from several studies supports the representation of the target in eye-centered coordinates (the point of origin is at the center of the gaze) in the posterior parietal cortex (PPC) in non-human primates [1], [2], [3], and in humans [4], [5]. In contrast, the brain transforms reaching planning into muscle activations in the shoulder-centered coordinates (the point of origin is at the shoulder) in the sensorimotor area (SMA) [6]. The question remains in which coordinates the brain computes the displacement vector necessary for reaching. Three theories arise: the brain could compute the displacement vector in the shoulder-centered, eye-centered coordinates, or other intermediate coordinates [5], [7].

Several electroencephalographic (EEG) studies provide strong evidence supporting that the information regarding hand kinematics is represented primarily in a low-frequency EEG in discrete reaching [8], [9], [10] and continuous tracking [11], [12], [13], [14], [15], [16]. Recent studies have also investigated other important aspects of hand kinematics decoding, which could improve the usability of the system: learning effect and adaptation over sessions [17], [18], decoding performance [19], and continuous error processing [20]. As proven useful in the majority of the study, we would like to focus on low-frequency EEG.

Let us consider inward and outward reachings of the same direction where the eyes are always fixated on the target prior to the initiation of the movement. The internally estimated displacement from hand to the target should always point towards the origin of the eye-centered coordinates and the reaching is done towards the target, regardless of the direction of reaching. On the other hand, the displacement should be represented differently in the shoulder-centered coordinates as the inward and outward displacement are represented with different sets of kinematics. We hypothesize that the the low-frequency EEG does not carry enough information to distinguish the inward and outward conditions, which also implies weakly that the reach planning is represented in eye-centered coordinates in low-frequency EEG. If this is the case, then a classifier should distinguish the inward and outward conditions with accuracy no better than chance. To answer this, we performed a preliminary study where we collected EEG from five healthy participants performing directional with inward and outward reaching.

MATERIALS AND METHODS

The experiment was designed based on discrete center-out reaching in 4 directions (up, down, left, and right). Participants performed outward reaching in one direction (e.g., left direction from center) and then inward reaching in the opposite direction (e.g., right direction to center) while fixating their eyes on the target (see Fig. 1c and d). When contrasting the inward and outward reaching from the same direction (e.g., right inward and right outward), the target will always be at the center of the eye-centered coordinates, while the hand position will be in different locations in the shoulder-centered coordinates.

Participants: In this preliminary study, data from five healthy participants (1 female) were recorded.

Published by
Verlag der Technischen Universität Graz

10.3217/978-3-99161-014-4-022

Three were right-handed, and two were ambidextrous, who normally used their right hand to control a computer mouse. The age range was between 30 ± 3.16 years old (mean ± std).

Biosignal recording: We measured 60 EEG channels and 4 electrooculogram (EOG) channels with a sampling frequency of 500 Hz using BrainAmp amplifiers (Brain Products GmbH, Gilching, Germany). The ground electrode was placed at Fpz, while the reference electrode was placed at the right mastoid. The EOG electrodes were positioned on the outer canthi of both eyes, above and under the left eye.

Hand movement recording: A custom-made motion capture system was employed to track hand position via a marker attached to the index finger, and a camera recorded at 30 Hz. The hand position was mapped to the cursor position so that the space between each grid marker (see Fig. 1) was roughly equal to 5cm on the physical plane. Additionally, the hand position was utilized in real time to estimate the direction of the movement. The detected direction of hand movement was used to provide feedback during the trial.

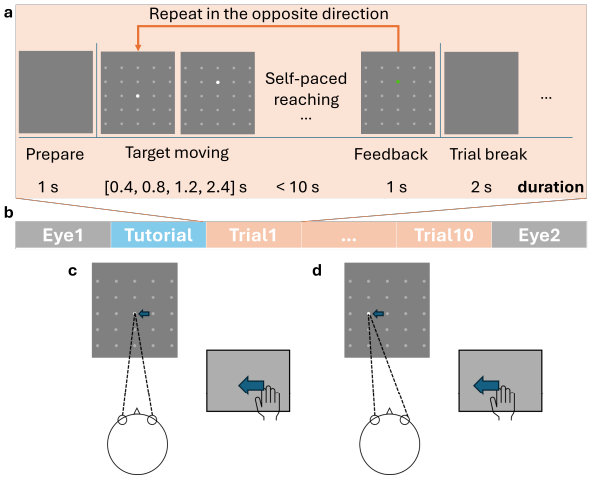

Figure 1: Overview of the experiment (a) timing of a trial, (b) structure of the experiment, (c) and (d) example of left directional reaching from the inward (c) and outward conditions (d) the grey block indicates a motion capture box used in the experiment.

Experimental paradigm: The overview of the experiment is visualized in Fig. 1. The experiment was divided into 13 blocks: 2 Eye blocks, 1 Tutorial block, and 10 Trial blocks. For the eye blocks, participants were asked to blink, move their eyes, or rest according to the visual cue. The data was used to correct the eye artifacts in the trial blocks, according to [21]. Another eye block was repeated at the end of the experiment.

During the tutorial, participants practiced reaching in different conditions. The participants were instructed to fixate their eyes on the target before initiating the reaching. The hand position was visualized only during the tutorial so that the participants got used to moving in 2 levels of distance. During the trial blocks, the task was to perform reaching conditions indicated by the target's movement. There were 4 directions (up, down, left, and right), 2 levels of speed (slow and quick), and 2 levels of distance (near and far), which summed up to 16 different reaching conditions. At the beginning of the trial, a blank screen was visualized for 1 s, indicating a preparation phase. Then, a 5-by-5 grid and a white circle ("target") at the center position appeared. The distance between each dot on the grid was calibrated to match 5 cm in real space, but the hand position was not shown to the participants to force them to always look at the target. The grid provided a guide on possible positions the target could move to (see Fig. 1a). The conditions of the reaching (direction, speed, distance) were randomized for each trial. The direction determined which direction the target moved toward; the speed determined how fast the target moved for 1 grid unit, either within 0.4 s for quick or 1.2 s for slow condition; the distance determined how far the target moved, either 1 or 2 grid units. The time required to move in the far condition was double that required in the near condition (e.g., 0.4 s in the quick near condition but 0.8 s in the quick far condition). As soon as the target stopped moving, the participants were instructed to wait for at least 1 s before initiating the same movement. The color of the target gave feedback: green for the correct direction of the hand movement within 10 s, or red for incorrect (wrong direction, no movement detected within 10 s). The feedback was given for 1 s before the target turned to white, prompting the preparation phase for the participants. The target then moved at the same distance and speed but in the opposite direction, towards the center position. The participants then waited for at least 1 s before initiating movement toward the center position. The feedback was given again for 1 s, and then the screen turned blank, indicating the trial break period. There were 480 trials (48 trials per block) but 960 movements because each trial comprised 2 movements (outward and inward). For simplicity, we treated outward and inward movements as separate trials, so the total number of trials is 960 trials. There were 480 trials for inward and outward conditions and 240 for direction conditions. On average, 157.2 ± 88.35 (mean ± SD) trials were rejected due to artifacts, incorrectly performed direction, distance, and speed.

Processing pipeline: The measured EEG and EOG signals were processed via a custom script based on EEGLAB [22] on MATLAB version R2019b. The EEG signals were visually inspected, and the bad channels were identified and interpolated. The powerline noise at 50 Hz was removed via 2nd order Butterworth notch filter. The signals were downsampled to 200 Hz and then bandpass filtered via the 2nd order Butterworth filter between 0.3 – 70 Hz. Eye artifacts were corrected via sparse generalized eye artifact subspace subtraction (SGEYESUB) [21], trained on the eye blocks data. Independent component analysis (ICA) was employed via the FastICA algorithm [23] to identify and remove the artifact component. The IClabel plugin was utilized to estimate the probability of each IC component being the artifact. Any IC components that had the probability

Published by
Verlag der Technischen Universität Graz

10.3217/978-3-99161-014-4-022

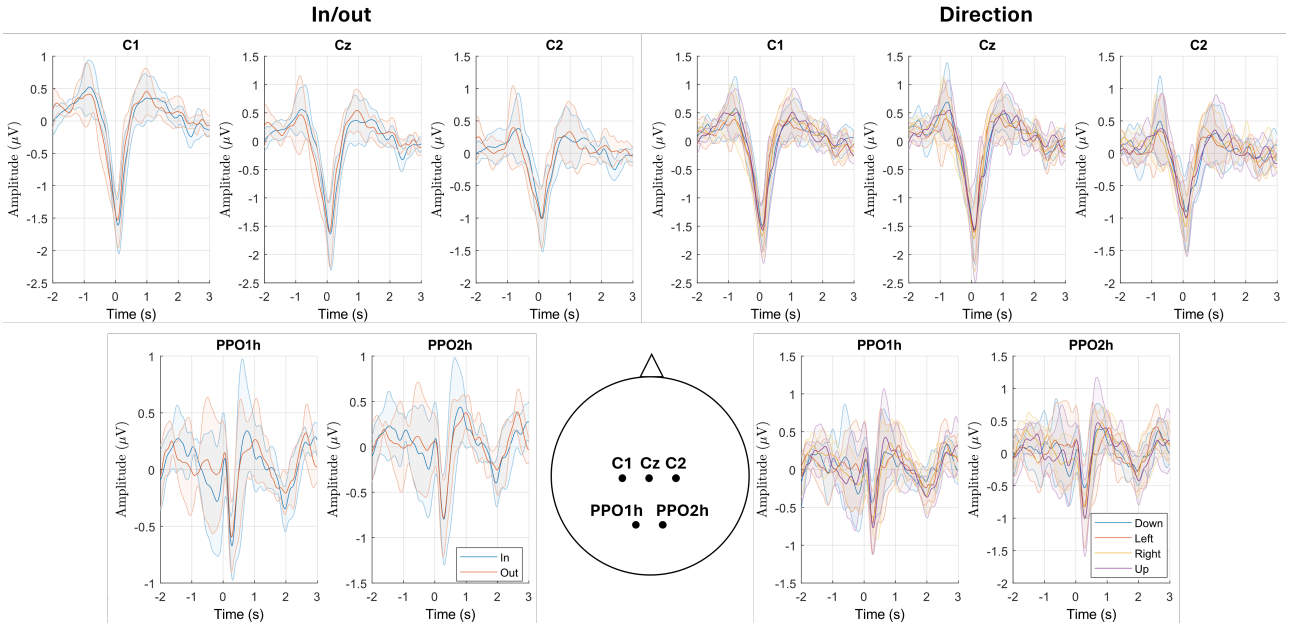

Figure 2: Average MRCP from C1, Cz, C2, PPO1h, and PPO2h in inward/outward and direction conditions. The shaded bands indicate standard deviation (SD) across participants.

of being any non-brain activity higher than 90% were removed and the cleaned signals were recomputed again. The EOG signals were included in the computation of the ICA to aid the identification of the eye artifact. The signals were epoched between -2 to 5 s around when the target stopped, and bad trials were identified based on the amplitude (rejected if amplitude was higher than ± 150 μV) and the statistics of the signals (joint probability, kurtosis). After trial rejection, signals were then low pass filtered with 2nd order Butterworth filter at 3 Hz and then epoched around the detected movement onsets between -3 to 3 s. The signals were then re-referenced to a common average reference (CAR).

Movement onset detection: The position of the hand was smoothened with a 1st-order Savitzky-Golay filter. The speed was computed by taking the derivative of the vector norm of the smoothened position in 2D. The onsets were detected when the speed exceeded the threshold at 30 pixels per second. The signals were epoched around these movement onsets, and the maximum movement speed and total distance were computed per movement. The median of the maximum speed across all movements was used as a threshold to identify bad movements (too fast or too slow for the speed conditions).

Similarly, the median of the total distance was used to classify bad movements (too far or too near for the distance conditions). Short movement (lasting less than 0.2 s), movement with "incorrect" feedback, and movement outside the movement period were excluded. Finally, the movements that were performed too soon (less than 0.5 s after the target stopped) were excluded as well. On average, 19.60 ± 14.04 trials were rejected due to incorrect behavior (e.g., no movement detected, wrong direction), while 61.80 ± 37.10 and 55.40 ± 59.25 trials were rejected due to incorrect distance and speed, respectively.

Movement-related cortical potential (MRCP) analysis: The signals were averaged over the same conditions in directions and inward/outward time-locked to the movement onset. The distance and speed were excluded from further analysis. The MRCPs were averaged over participants, but no statistical tests were performed due to the low number of participants.

Point-wise Classification: A shrinkage linear discriminant analysis (sLDA) [24] was employed for classification. Only the EEG signals were considered in this case. AF row channels were excluded due to the residual artifacts that could not be corrected from the eye artifact correction model. The signals were downsampled to 10 Hz to reduce the computational time. The input features for the training were the amplitude of EEG signals within a sliding window with a size between 1 sample (spontaneous) and 10 samples (1-s windows). Due to the maximum window size, the first second of the trial was omitted from the classification. We tested the classification on directions and inward/outward conditions. An sLDA model was trained per time point, so there were 51 sLDA models per condition. The training of each model was done with stratified 10-fold cross-validation. To estimate the effect of the classification, the chance level was simulated with a label shuffling approach [25] according to the number of classes and number of trials per class (TPC). In the direction case, the chance level was determined with 4 classes with 240 TPCs, and in the inward/outward, with 2 classes with 480 TPCs. No statistical tests were performed due to the low number of participants.

RESULTS

MRCP analysis: The shape of MRCPs of different directions and inward/outward conditions is illustrated in Fig. 2. In both the direction and inward/outward

Published by
Verlag der Technischen Universität Graz

10.3217/978-3-99161-014-4-022

conditions, the amplitude of the MRCPs was strongest at Cz and C1 channels. The minimum peaks in PPO1h and PPO2h lagged behind the ones in C1, Cz, and C2 by 200 ms. The shape of MRCPs differed in C1, Cz, and C2 but not in PPO1h and PPO2h. Only the amplitude of the minimum peaks in the PPO1h and PPO2h differed slightly. Similar effects could also be seen in the direction conditions. Additionally, the shape of MRCPs was similar in the horizontal (left and right) and vertical directions (up and down).

Point-wise classification: Fig. 3 visualizes the classification accuracy of the direction and the inward/outward condition. The estimated chance level was determined to be 27.39% and 52.70% for the direction and inward/outward conditions, respectively. In the inward/outward conditions, the average accuracy hovered around the chance level. The peak accuracy was around 0.3 s at 55.53% for the spontaneous classification and at 0 s at 58.16% for 1 s window classification. On the other hand, the accuracy curve of the direction stayed around the chance level before rising well beyond it and then peaks at 0.6 s at 34.24% for the spontaneous classification and at 0.9 s at 40.59% for the 1 s window classification after movement onset and then dips below the chance level again after 1s. The accuracy generally improved with increasing window size.

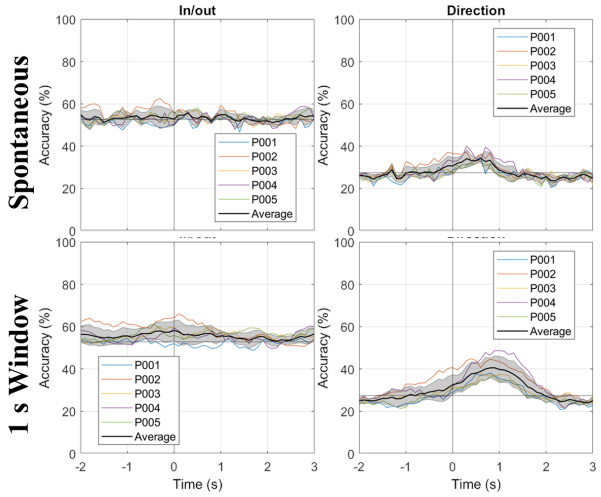

Figure 3: Accuracy curve from spontaneous and 1-s window point-wise classification. Each line indicates the accuracy of each participant. The black line and the shaded area indicate the average accuracy over 5 participants and ± standard deviation (SD)

DISCUSSION

The results suggested that the low-frequency EEG does not carry enough information to distinguish between inward and outward conditions, whereas the amount of information seemed to suffice to distinguish the direction of reaching, as seen in Fig. 3. This seemed to support the hypothesis that the low-frequency EEG carries information that is likely to be represented in the eye-centered coordinates.

Interestingly, we observed in the inward and outward conditions the similar shape of the MRCP in PPO1h and PPO2h, whereas the shape differed slightly in the C1, Cz, and C2. As discussed earlier, the main difference between inward and outward conditions was in the different representations of the planned displacement vector in the shoulder-centered but not in the eye-centered coordinates. We speculated that this could be related to the underlying referencing frame in shoulder-centered coordinates in SMA [6] (represented as C1, Cz, and C2) and in eye-centered coordinates in PPC [1] (represented as PPO1h and PPO2h). However, we must be careful in drawing any strong conclusion on this topic due to the low number of participants and the lack of evidence linking the non-invasive and EEG measurements.

On the other hand, the directional information of the reaching seemed to be well represented in the EEG signal. The different shapes of MRCP in the horizontal (up and down) and vertical reaching (left and right) could be explained by the different muscle/joint activations when reaching in the left and right in comparison to the up and down direction. Alternatively, this could be due to a mismatch in the actual plane of the movement and the plane of the screen in up and down directions (as the left and right were correspondingly in the same plane) [16], [19]. Nevertheless, the directional information of the reaching could be distinguished with above-chance accuracy.

For further analysis in a subsequent study, the data from the inward and outward can safely be combined. The model showed promising peak accuracy for the direction at 40.59%, which was lower than the accuracy reported in similar directional decoding studies [8], [9], [10]. The classification in this study only represented how informative each time point was in discriminating between conditions but did not reflect the actual decoding accuracy of the detection of the directional reaching. Another major difference was that the participants were specifically asked to fixate their eyes on the target so that the eye movement was completely separated from the movement. This might reduce the amount of information that the decoder could utilize. Further analysis with more participants would be needed to draw a stronger conclusion.

CONCLUSION

We provided a preliminary result that low-frequency EEG may be globally represented in the eye-coordinates. We speculated that the shape of MRCP in PPC and SMA may represent the underlying referencing frames as reported in earlier studies. The classification results also confirmed that the directional information was encoded in the movement planning, which was sufficient to differentiate between directions but suggested that the inward and outward movement were not differentiable and could be combined for further analysis.

ACKNOWLEDGEMENTS

We thank Markus Crell for the hand motion-capturing system. We would like to thank the Graz BCI

Published by
Verlag der Technischen Universität Graz

10.3217/978-3-99161-014-4-022

Team, especially Hannah Pulferer and Markus Crell, for fruitful discussions. NS received funding from the Royal Thai Government.

REFERENCES

[1] A. P. Batista, C. A. Buneo, L. H. Snyder, and R. A. Andersen, "Reach Plans in Eye-Centered Coordinates," *Science*, vol. 285, no. 5425, pp. 257–260, Jul. 1999, doi: 10.1126/science.285.5425.257.

[2] C. A. Buneo, M. R. Jarvis, A. P. Batista, and R. A. Andersen, "Direct visuomotor transformations for reaching," *Nature*, vol. 416, no. 6881, Art. no. 6881, Apr. 2002, doi: 10.1038/416632a.

[3] A. Battaglia-Mayer *et al.*, "Early Coding of Reaching in the Parietooccipital Cortex," *J. Neurophysiol.*, vol. 83, no. 4, pp. 2374–2391, Apr. 2000, doi: 10.1152/jn.2000.83.4.2374.

[4] S. M. Beurze, S. Van Pelt, and W. P. Medendorp, "Behavioral Reference Frames for Planning Human Reaching Movements," *J. Neurophysiol.*, vol. 96, no. 1, pp. 352–362, Jul. 2006, doi: 10.1152/jn.01362.2005.

[5] J. D. Crawford, W. P. Medendorp, and J. J. Marotta, "Spatial Transformations for Eye–Hand Coordination," *J. Neurophysiol.*, vol. 92, no. 1, pp. 10–19, Jul. 2004, doi: 10.1152/jn.00117.2004.

[6] S. Kakei, D. S. Hoffman, and P. L. Strick, "Sensorimotor transformations in cortical motor areas," *Neurosci. Res.*, vol. 46, no. 1, pp. 1–10, May 2003, doi: 10.1016/S0168-0102(03)00031-2.

[7] R. Shadmehr and S. P. Wise, *The Computational Neurobiology of Reaching and Pointing: A Foundation for Motor Learning*. in Computational Neuroscience Series. MIT Press, 2004.

[8] S. Waldert *et al.*, "Hand Movement Direction Decoded from MEG and EEG," *J. Neurosci.*, vol. 28, no. 4, pp. 1000–1008, Jan. 2008, doi: 10.1523/JNEUROSCI.5171-07.2008.

[9] R. J. Kobler, E. Kolesnichenko, A. I. Sburlea, and G. R. Müller-Putz, "Distinct cortical networks for hand movement initiation and directional processing: An EEG study," *NeuroImage*, vol. 220, p. 117076, Oct. 2020, doi: 10.1016/j.neuroimage.2020.117076.

[10] V. Shenoy Handiru, A. P. Vinod, and C. Guan, "EEG source space analysis of the supervised factor analytic approach for the classification of multi-directional arm movement," *J. Neural Eng.*, vol. 14, no. 4, p. 046008, Aug. 2017, doi: 10.1088/1741-2552/aa6baf.

[11] T. J. Bradberry, R. J. Gentili, and J. L. Contreras-Vidal, "Reconstructing Three-Dimensional Hand Movements from Non-invasive Electroencephalographic Signals," *J. Neurosci.*, vol. 30, no. 9, pp. 3432–3437, Mar. 2010, doi: 10.1523/JNEUROSCI.6107-09.2010.

[12] A. Korik, R. Sosnik, N. Siddique, and D. Coyle, "Imagined 3D Hand Movement Trajectory Decoding from Sensorimotor EEG Rhythms," presented at the 2016 IEEE International Conference on Systems, Man and Cybernetics, 2016, p. 7.

[13] B. J. Edelman *et al.*, "Non-invasive neuroimaging enhances continuous neural tracking for robotic device control," *Sci. Robot.*, vol. 4, no. 31, p. eaaw6844, Jun. 2019, doi: 10.1126/scirobotics.aaw6844.

[14] V. Mondini, R. J. Kobler, A. I. Sburlea, and G. R. Müller-Putz, "Continuous low-frequency EEG decoding of arm movement for closed-loop, natural control of a robotic arm," *J. Neural Eng.*, Jul. 2020, doi: 10.1088/1741-2552/aba6f7.

[15] R. J. Kobler, A. I. Sburlea, V. Mondini, M. Hirata, and G. R. Müller-Putz, "Distance- and speed-informed kinematics decoding improves M/EEG based upper-limb movement decoder accuracy," *J. Neural Eng.*, Aug. 2020, doi: 10.1088/1741-2552/abb3b3.

[16] V. Martınez-Cagigal, R. J. Kobler, V. Mondini, R. Hornero, and G. R. Müller-Putz, "Non-Linear Online Low-Frequency EEG Decoding of Arm Movements During a Pursuit Tracking Task," in *2020 42nd Annual International Conference of the IEEE Engineering in Medicine Biology Society (EMBC)*, 2020, p. 5. doi: 10.1109/EMBC44109.2020.9175723.

[17] H. S. Pulferer, B. Ásgeirsdóttir, V. Mondini, A. I. Sburlea, and G. R. Müller-Putz, "Continuous 2D trajectory decoding from attempted movement: across-session performance in able-bodied and feasibility in a spinal cord injured participant," *J. Neural Eng.*, vol. 19, no. 3, p. 036005, Jun. 2022, doi: 10.1088/1741-2552/ac689f.

[18] N. Srisrisawang and G. R. Müller-Putz, "Transfer Learning in Trajectory Decoding: Sensor or Source Space?," *Sensors*, vol. 23, no. 7, p. 3593, Mar. 2023, doi: 10.3390/s23073593.

[19] N. Srisrisawang and G. R. Müller-Putz, "Applying Dimensionality Reduction Techniques in Source-Space Electroencephalography via Template and Magnetic Resonance Imaging-Derived Head Models to Continuously Decode Hand Trajectories," *Front. Hum. Neurosci.*, vol. 16, p. 830221, Mar. 2022, doi: 10.3389/fnhum.2022.830221.

[20] H. S. Pulferer, K. Kostoglou, and G. R. Müller-Putz, "Getting off track: Cortical feedback processing network modulated by continuous error signal during target-feedback mismatch," *NeuroImage*, vol. 274, p. 120144, Jul. 2023, doi: 10.1016/j.neuroimage.2023.120144.

[21] R. J. Kobler, A. I. Sburlea, C. Lopes-Dias, A. Schwarz, M. Hirata, and G. R. Müller-Putz, "Corneo-retinal-dipole and eyelid-related eye artifacts can be corrected offline and online in electroencephalographic and magnetoencephalographic signals," *NeuroImage*, vol. 218, p. 117000, Sep. 2020, doi: 10.1016/j.neuroimage.2020.117000.

[22] A. Delorme and S. Makeig, "EEGLAB: an open

Published by
Verlag der Technischen Universität Graz

10.3217/978-3-99161-014-4-022

source toolbox for analysis of single-trial EEG dynamics including independent component analysis," *J. Neurosci. Methods*, vol. 134, no. 1, pp. 9–21, Mar. 2004, doi: 10.1016/j.jneumeth.2003.10.009.

[23] A. Hyvärinen and E. Oja, "Independent component analysis: algorithms and applications," *Neural Netw.*, vol. 13, no. 4, pp. 411–430, Jun. 2000, doi: 10.1016/S0893-6080(00)00026-5.

[24] B. Blankertz, S. Lemm, M. Treder, S. Haufe, and K.-R. Müller, "Single-trial analysis and classification of ERP components — A tutorial," *NeuroImage*, vol. 56, no. 2, pp. 814–825, May 2011, doi: 10.1016/j.neuroimage.2010.06.048.

[25] G. R. Müller-Putz, R. Scherer, C. Brunner, R. Leeb, and G. Pfurtscheller, "Better than random? A closer look on BCI results," *Int. J. Bioelectromagn.*, vol. 10, no. 1, pp. 52–55, 2008.

Published by
Verlag der Technischen Universität Graz